November 1996 LIDS-P-2370

Research Supported By:

AFOSR grant F49620-95-1-0083
ONR grant N00014-91-J-1004
Boston Univ. GC123919NGD

SCALE SPACE ANALYSIS BY STABILIZED INVERSE DIFFUSION EQUATIONS

Ilya Pollak, Alan S. Willsky, Hamid Krim

Scale Space Analysis by Stabilized Inverse Diffusion Equations.[1]

Ilya Pollak[2]
e-mail: ipollak@mit.edu, tel: 617-253-3816, fax: 617-258-8553, Room 35-427
Alan S. Willsky
Hamid Krim

Abstract. We introduce a family of first-order multi-dimensional ordinary differential equations (ODEs) with discontinuous right-hand sides and demonstrate their applicability in image processing. An equation belonging to this family is an inverse diffusion everywhere except at local extrema, where some stabilization is introduced. For this reason, we call these equations "stabilized inverse diffusion equations" ("SIDEs"). A SIDE in one spatial dimension may be interpreted as a limiting case of a semi-discretized Perona-Malik equation [3, 4]. In an experimental section, SIDEs are shown to suppress noise while sharpening edges present in the input signal. Their application to image segmentation is demonstrated.

1 Introduction

In this paper we introduce, analyze, and apply a new class of nonlinear image processing algorithms. These algorithms are motivated by the great recent interest in using evolutions specified by partial differential equations (PDE's) as image processing procedures for tasks such as edge enhancement and segmentation, among others (see [1, 2, 6] and references therein). While the analysis of these techniques is most often performed in the continuous setting, where an image is identified with a function of two continuous spatial variables, the implementation of such equations generally involves their discrete approximation. As a consequence, as Weickert pointed out in [8], "a scale-space representation cannot perform better than its discrete realization". Following this suggestion, we concentrate in this paper on semi-discrete scale spaces (i.e., continuous in scale (or time) and discrete in space). More specifically, the main contribution of this paper is a new family of semi-discrete evolution equations which stably sharpen edges and suppress noise. The starting point for the development of these equations is a discrete interpretation of anisotropic diffusions such as that used by Perona-Malik [3, 4]. One motivation for such equations is precisely that of achieving both noise removal and edge enhancement through the use of a diffusion-like equation which in essence acts as an unstable inverse diffusion near edges and as a stable linear-heat-equation-like diffusion in homogeneous regions without edges. In a sense that we will make both conceptually clear and precise, the evolutions that we introduce may be viewed as a conceptually limiting case of such diffusions. These evolutions have discontinuous right-hand sides and act as inverse diffusions "almost everywhere" with stabilization resulting from the presence of the discontinuities in the vector field defined by the evolution. As we will see, the scale space of such an equation is a family

[1]The work of the authors was supported in part by AFOSR grant F49620-95-1-0083, ONR grant N00014-91-J-1004, and by subcontract GC123919NGD from Boston University under the AFOSR Multidisciplinary Research Program on Reduced Signature Target Recognition.

[2]The authors are affiliated with the Department of Electrical Engineering and Computer Science and the Laboratory for Information and Decision Systems at the Massachusetts Institute of Technology, 77 Massachusetts Avenue, Cambridge, MA 02139.

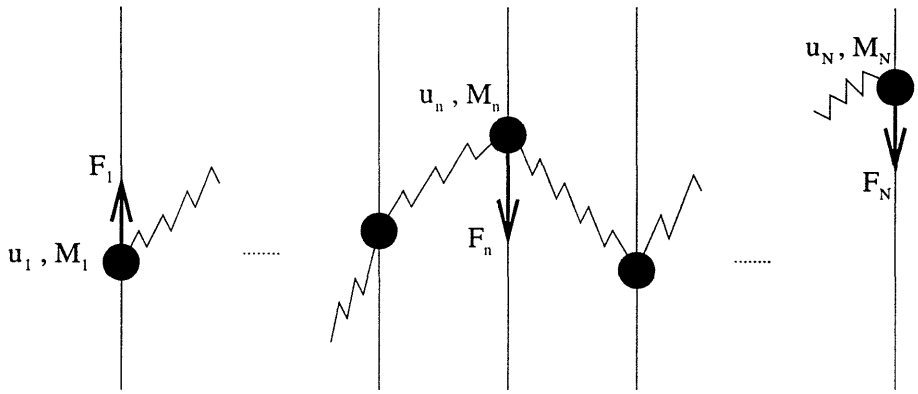

Figure 1: A spring-mass model.

of segmentations of the original image, with larger values of the scale parameter t corresponding to segmentations at coarser resolutions. Moreover, in contrast to continuous evolutions, those introduced here naturally define a sequence of logical "stopping times", i.e. points along the evolution fraught with useful information one may wish to extract, and corresponding to times at which the evolution hits a discontinuity surface of its solution field. These times are data-adaptive, i.e., they depend on the initial image, and result in a sequence of images at increasingly coarser resolutions, where the resolutions are adapted to the image being analyzed.

In the next section, we begin by describing a convenient mechanical analog for the visualization of many spatially-discrete evolution equations, including discretized linear or nonlinear diffusions such as that of Perona-Malik, as well as the discontinuous equations that we introduce in Section 3. Because of the discontinuous right-hand side, some care must be taken in defining solutions, but as we show in [5], once this is done, the resulting evolutions have a number of important properties. Moreover, as we have indicated, they lead to very effective algorithms for edge enhancement and segmentation, something that we demonstrate in Section 4. In particular, as we will see, they can produce sharp enhancement of edges in high noise as well as accurate segmentations of very noisy imagery such as synthetic aperture radar (SAR) imagery subject to severe speckle.

2 A Spring-Mass Model for Certain Evolution Equations

As we indicated in the introduction, the focus of this paper is on discrete-space, temporally-continuous evolutions of the following general form:

$$\begin{aligned} \dot{\mathbf{u}}(t) &= \mathcal{F}(\mathbf{u})(t), \\ \mathbf{u}(0) &= \mathbf{u}_0, \end{aligned} \tag{1}$$

where $\mathbf{u}$ is either a discretized signal, i.e., an N-point discrete sequence ($\mathbf{u} = (u_1, ..., u_N)^T \in \mathbb{R}^N$), or an N-by-N image whose j-th entry in the i-th row is u_{ij} ($\mathbf{u} \in \mathbb{R}^{N^2}$). The initial condition $\mathbf{u}_0$ corresponds to the original signal or image to be processed, and $\mathbf{u}(t)$ then represents the evolution of this signal/image at time (scale) t, resulting in a scale-space family for $0 \leq t < \infty$.

The nonlinear operators $\mathcal{F}$ of interest in this paper can be conveniently visualized through the following simple mechanical model. For the sake of simplicity in visualization, let us first suppose that $\mathbf{u} \in \mathbb{R}^N$ is a one-dimensional (1-D) sequence, and interpret

$\mathbf{u}(t) = (u_1(t), ..., u_N(t))^T$ in (1) as the vector of vertical positions of the N particles of masses $M_1, ..., M_N$, depicted in Figure 1. The particles are forced to move along N vertical lines. Each particle is connected by springs to its two neighbors (except the first and last particles, which are only connected to one neighbor.) Every spring whose vertical extent is v has energy $E(v)$, i.e., the energy of the spring between the n-th and $(n+1)$-st particles is $E(u_{n+1} - u_n)$. We impose the usual requirements for an energy function:

$$\begin{aligned} E(v) &\geq 0, \quad E(0) = 0, \\ E'(v) &\geq 0 \text{ for } v > 0, \\ E(v) &= E(-v). \end{aligned} \tag{2}$$

Then the derivative of $E(v)$, which we refer to as "the force function" and denote by $F(v)$, satisfies

$$\begin{aligned} F(0) &= 0, \quad F(v) \geq 0 \text{ for } v > 0, \\ F(v) &= -F(-v). \end{aligned} \tag{3}$$

We also call $F(v)$ a "force function" and $E(v)$ an "energy" if $-E(v)$ satisfies (2) and $-F(v)$ satisfies (3). We make the movement of the particles non-conservative by stopping it after a small period of time Δt and re-starting with zero velocity. We assume that during one such step, the total force $F_n = -F(u_n - u_{n+1}) - F(u_n - u_{n-1})$, acting on the n-th particle, stays approximately constant. The displacement during one iteration is equal to the product of acceleration and the square of the time interval, divided by two:

$$u_n(t + \Delta t) - u_n(t) = \frac{(\Delta t)^2}{2} \frac{F_n}{M_n}.$$

Letting $\Delta t \to 0$, while fixing $\frac{2M_n}{\Delta t} = m_n$, where m_n is a positive constant, leads to

$$\dot{u}_n = \frac{1}{m_n}(F(u_{n+1} - u_n) - F(u_n - u_{n-1})), \quad n = 1, 2, ..., N, \tag{4}$$

with the conventions $u_0 = u_1$ and $u_{N+1} = u_N$ imposed by the absence of springs to the left of the first particle and to the right of the last particle. We will refer to m_n as "the mass of the n-th particle" in the remainder of the paper. In the three examples below, we set $m_n = 1$.

We call $F(v)$ a "diffusion force" if, in addition to (3), it is monotonously increasing:

$$v_1 < v_2 \quad \Rightarrow \quad F(v_1) < F(v_2). \tag{5}$$

We call the corresponding energy $E(v)$ a "diffusion energy" and the corresponding evolution (4) a "diffusion". We call $F(v)$ an "inverse diffusion force" if $-F(v)$ satisfies Equations (3) and (5). The corresponding evolution (4) is called an "inverse diffusion". Inverse diffusions have the characteristic of enhancing abrupt differences in $\mathbf{u}$ corresponding to "edges" in the 1-D sequence. Such pure inverse diffusions, however, lead to unstable evolutions. The following example, which is prototypical of the examples considered by Perona and Malik, defines a stable evolution that captures at least some of the edge enhancing characteristics of inverse diffusions.

Example. Taking $F(v) = v \exp(-(\frac{v}{K})^2)$, as illustrated in Figure 2, yields a 1-D semi-discrete (continuous in scale and discrete in space) version of the Perona-Malik equation (see

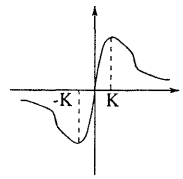

Figure 2: Force function for Perona-Malik evolution.

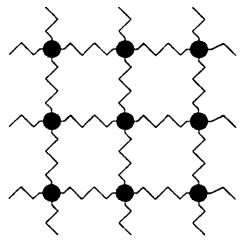

Figure 3: Spring-mass model in 2-D (view from above).

equations (3.3), (3.4), and (3.12) in [4]). In general, given a positive constant K, we call a force $F(v)$ a "Perona-Malik force of thickness K" if, in addition to (3), it satisfies the following conditions:

$$\begin{aligned} &F(v) \text{ has a unique maximum at } v = K, \\ &F(v_1) = F(v_2) \quad \Rightarrow \quad (|v_1| - K)(|v_2| - K) < 0. \end{aligned} \tag{6}$$

We call the corresponding energy a "Perona-Malik energy" and the corresponding evolution a "Perona-Malik evolution of thickness K". As Perona and Malik demonstrate (and as can also be inferred from our results), evolutions with such a force function act like inverse diffusions in the regions of high gradient and like usual diffusions elsewhere. They are stable and capable of achieving some level of edge enhancement depending on the exact form of $F(v)$. ■

Finally, to extend our mechanical model of Figure 1 to images, we simply replace the sequence of vertical lines along which the particles move with an N-by-N square grid of such lines. The particle at location (i, j) is connected by springs to its four neighbors: $(i-1, j)$, $(i, j+1)$, $(i+1, j)$, $(i, j-1)$, except for the particles in the four corners of the square (which only have two neighbors each), and the rest of the particles on the boundary of the square (which have three neighbors). The view from above of this arrangement is depicted in Figure 3. It is reminiscent of (and, in fact, was suggested by) the resistive network of Figure 8 in [3]. The analog of the equation (4) for images is then:

$$\dot{u}_{ij} = \frac{1}{m_{ij}}(F(u_{i+1,j} - u_{ij}) - F(u_{ij} - u_{i-1,j}) + F(u_{i,j+1} - u_{ij}) - F(u_{ij} - u_{i,j-1})), \tag{7}$$

with $i = 1, 2, ..., N$, $j = 1, 2, ..., N$, and the conventions $u_{0,j} = u_{1,j}$, $u_{N+1,j} = u_{N,j}$, $u_{i,0} = u_{i,1}$ and $u_{i,N+1} = u_{i,N}$ imposed by the absence of springs outside of $1 \le i \le N$, $1 \le j \le N$.

3 Stabilized Inverse Diffusion Equations (SIDEs)

In this section, we introduce a discontinuous force function, resulting in a system (4) that has discontinuous right-hand side (RHS). Such equations received much attention in control theory because of the wide usage of relay switches in automatic control systems. More recently,

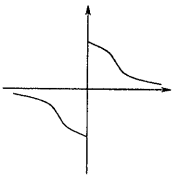

Figure 4: Force function for a stabilized inverse diffusion.

deliberate introduction of discontinuities has been used in control applications to drive the state vector onto lower-dimensional surfaces in the state space [7]. As we will see, this objective of driving a trajectory onto a lower-dimensional surface also has value in image analysis and in particular in image segmentation. Segmenting a signal or image, represented as a high-dimensional vector $\mathbf{u}$, consists of evolving it so that it is driven onto a comparatively low-dimensional subspace which corresponds to a segmentation of the signal or image domain into a small number of regions.

The type of force function of interest to us here is illustrated in Figure 4. More precisely, we wish to consider force functions $F(v)$ which, in addition to (3), satisfy the following properties:

$$\begin{aligned} F'(v) \leq 0 \quad &\text{for} \quad v \neq 0, \\ F(0^+) > 0, \quad & \\ F(v_1) = F(v_2) \quad &\Leftrightarrow \quad v_1 = v_2. \end{aligned} \tag{8}$$

Contrasting this form of a force function to the Perona-Malik function in Figure 2, we see that in a sense one can view the discontinuous force function as a limiting form of the continuous force function in Figure 2. In essence, this new force function acts as an inverse diffusion operator as long as its argument is not zero. This would appear, at first, to lead to potential problems, since the way in which Perona-Malik-type equations achieve stability is through the positive diffusion effects resulting from the behavior of $F(v)$ for $v \in [-K, K]$. More fundamentally, because of the discontinuity at the origin of the force function in Figure 4, there is a question of how one defines solutions of the equation (4) for such a force function. Indeed, if the equation (4) evolves toward a point of discontinuity of its RHS, the value of the RHS of (4) apparently depends on the direction from which this point is approached (because $F(0^+) \neq F(0^-)$), making further evolution non-unique. We therefore need a special definition of how the trajectory of our evolution proceeds at these discontinuity points.[3] For this definition to be useful, the resulting evolution must satisfy well-posedness properties: the existence and uniqueness of solutions, as well as stability of solutions with respect to the initial data. In the rest of this section, we describe how we define solutions to (4) for force functions (8). Assuming the resulting evolutions to be well-posed, we demonstrate that they have the qualitative properties we desire, namely that they both are stable and also act as inverse diffusions and hence enhance edges. We address the issue of well-posedness and other properties in [5].

Consider the evolution (4) with $F(v)$ as in Figure 4 and Eq. (8) and with all of the masses m_n equal to 1. Notice that the RHS of (4) has a discontinuity at a point $\mathbf{u}$ if and only if $u_i = u_{i+1}$ for some i between 1 and $N-1$. It is when a trajectory reaches such a point $\mathbf{u}$

[3]Having such a definition is crucial because, as we show in [5], equation (4) will reach a discontinuity point of its RHS in finite time, starting with any initial condition.

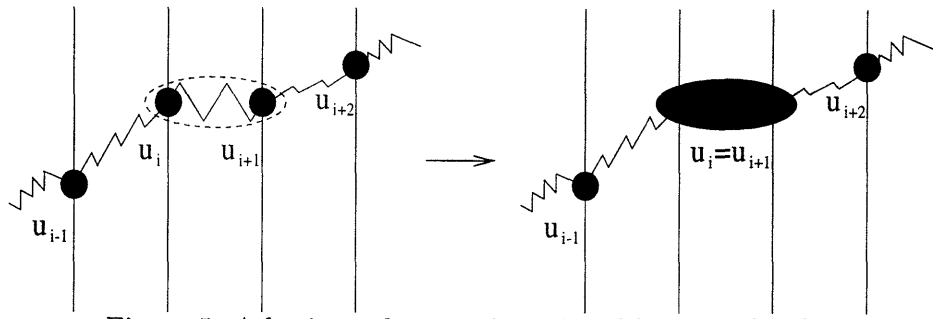

Figure 5: A horizontal spring is replaced by a rigid link.

that we need the following definition. In terms of our spring-mass model of Figure 1, once the vertical positions u_i and u_{i+1} of two neighboring particles become equal, the spring connecting them is replaced by a rigid link. In other words, the two particles are simply merged into a single particle which is twice as heavy (see Figure 5), yielding the following modification of (4) for $n = i$ and $n = i + 1$:

$$\dot{u}_i = \dot{u}_{i+1} = \frac{1}{2}((F(u_{i+2} - u_{i+1}) - F(u_i - u_{i-1})).$$

(The differential equations for $n \neq i, i+1$ do not change.) Similarly, if m consecutive particles reach equal vertical position, they are merged into one particle of mass m ($1 \leq m \leq N$):

$$\dot{u}_n = ... = \dot{u}_{n+m-1} = \frac{1}{m}(F(u_{n+m} - u_{n+m-1}) - F(u_n - u_{n-1})) \tag{9}$$
$$\text{if} \quad u_{n-1} \neq u_n = u_{n+1} = ... = u_{n+m-2} = u_{n+m-1} \neq u_{n+m}.$$

Notice that this system is the same as (4), but with possibly unequal masses. It is convenient to re-write this equation so as to explicitly indicate the reduction in the number of state variables:

$$\dot{u}_{n_i} = \tfrac{1}{m_{n_i}}(F(u_{n_{i+1}} - u_{n_i}) - F(u_{n_i} - u_{n_{i-1}})), \tag{10}$$
$$u_{n_i} = u_{n_i+1} = ... = u_{n_i+m_{n_i}-1},$$
$$\text{where } i = 1, ..., p,$$
$$1 = n_1 < n_2 < ... < n_{p-1} < n_p \leq N,$$
$$n_{i+1} = n_i + m_{n_i}.$$

The compound particle described by the vertical position u_{n_i} and mass m_{n_i} consists of m_{n_i} unit-mass particles u_{n_i}, u_{n_i+1}, ..., $u_{n_i+m_{n_i}-1}$ that have been merged, as shown in Figure 5. The evolution can then naturally be thought of as a sequence of stages: during each stage, the right-hand side of (10) is continuous. Once the solution hits a discontinuity surface of the right-hand side, the state reduction and re-assignment of m_{n_i}'s, described above, takes place. The solution then proceeds according to the modified equation until it hits the next discontinuity surface, etc. The definition of SIDEs in 2-D is similar; it is given in [5].

We close this section by describing one of the basic and most important properties of these evolutions, namely that the evolution is stable but nevertheless behaves like an inverse diffusion. Notice that a force function $F(v)$ satisfying (8) can be represented as the sum of an inverse diffusion force $F_{id}(v)$ and a positive multiple of sign(v):

$$F(v) = F_{id}(v) + C\,\text{sign}(v),$$

where $C = F(0^+)$ and $-F_{id}(v)$ satisfies (3) and (5). Therefore, if $u_{n_{i+1}} - u_{n_i}$ and $u_{n_i} - u_{n_{i-1}}$ are of the same sign (which means that u_{n_i} is not a local extremum of the sequence $(u_{n_1}, ..., u_{n_p})$), then (10) can be written as

$$\dot{u}_{n_i} = \frac{1}{m_{n_i}}(F_{id}(u_{n_{i+1}} - u_{n_i}) - F_{id}(u_{n_i} - u_{n_{i-1}})). \tag{11}$$

If $u_{n_i} > u_{n_{i+1}}$ and $u_{n_i} > u_{n_{i-1}}$ (i.e., u_{n_i} is a local maximum), then (10) is

$$\dot{u}_{n_i} = \frac{1}{m_{n_i}}(F_{id}(u_{n_{i+1}} - u_{n_i}) - F_{id}(u_{n_i} - u_{n_{i-1}}) - 2C). \tag{12}$$

If $u_{n_i} < u_{n_{i+1}}$ and $u_{n_i} < u_{n_{i-1}}$ (i.e., u_{n_i} is a local minimum), then (10) is

$$\dot{u}_{n_i} = \frac{1}{m_{n_i}}(F_{id}(u_{n_{i+1}} - u_{n_i}) - F_{id}(u_{n_i} - u_{n_{i-1}}) + 2C). \tag{13}$$

Equation (11) says that the evolution is a pure inverse diffusion at the points which are not local extrema. It is not, however, a *global* inverse diffusion, since pure inverse diffusions drive local maxima to $+\infty$ and local minima to $-\infty$ and thus are unstable. In contrast, equations (12) and (13) show that at local extrema, our evolution is an inverse diffusion plus a stabilizing term which guarantees that the local maxima do not increase and the local minima do not decrease. For this reason, we call the new evolution (10) a "stabilized inverse diffusion equation" ("SIDE"), a force function satisfying (8) a "SIDE force", and the corresponding energy a "SIDE energy".

4 Experiments

The examples below are generated with the following SIDE force function:

$$\begin{aligned} F(v) &= 1 - \tfrac{v}{L} \qquad \text{if} \quad 0 < v \leq L, \\ F(v) &= -1 - \tfrac{v}{L} \qquad \text{if} \quad -L \leq v < 0, \end{aligned}$$

where $L/2$ is greater than the maximum of the absolute value of the initial condition[4].

4.1 Experiment 1: SIDE evolutions in 1-D

We first test this SIDE on a unit step function corrupted by additive white Gaussian noise whose standard deviation is equal to the amplitude of the step. The noise-free unit step is shown in Figure 6(a), while the noise-corrupted measurement of the step is depicted in Figure 6(b). The remaining parts of this figure display snapshots of the SIDE evolution starting with the noisy data in Figure 6(b). The particular members of the scale space which are illustrated are labeled according to the number of remaining regions (i.e., what we called "compound particles" in the preceding section). Note that the last remaining edge, i.e., the edge in Figure 6(f) for the time at which there are only two regions left, is located between samples 96 and 97, which is quite close to the position of the original edge (between the 100-th and 101-st

[4]Thanks to the maximum principle proved in [5], the absolute value of the argument of F is never larger than L during the evolution. Consequently, it does not matter what $F(v)$ is for $v \notin [-L; L]$.

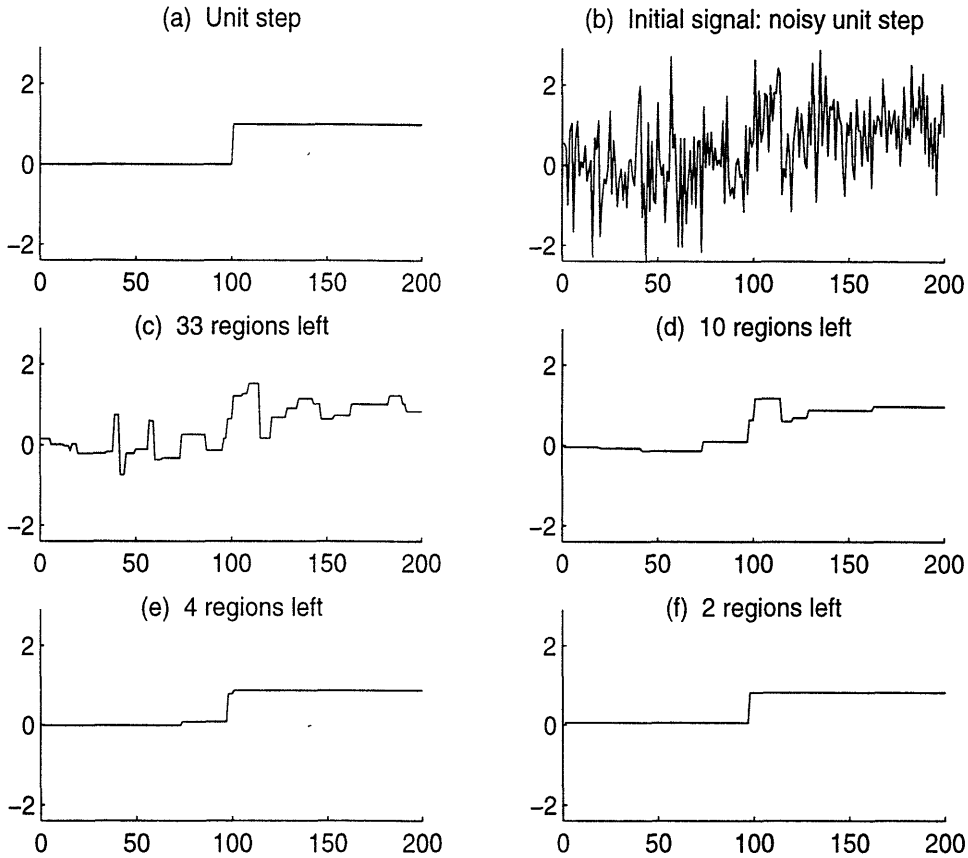

Figure 6: Scale space of a SIDE for a noisy step: (a) unit step; (b) its noisy realization; (c)–(f) representatives of the resulting SIDE scale space.

samples). In this example, the step in Figure 6(f) also has amplitude that is close to that of the original unit step. In general, thanks to the stability of SIDEs, the sizes of discontinuities will be diminished through such an evolution, much as they are in other evolution equations. However, from the perspective of segmentation this is irrelevant–i.e., the focus of attention is on detecting and locating the edge, not on estimating its amplitude–and that is the aspect on which we wish to focus here.

This example also provides us with the opportunity to contrast the behavior of a SIDE evolution with a Perona-Malik evolution and in fact to describe the behavior that originally motivated our work. Specifically, as we note in [5], a SIDE in 1-D can be approximated with a Perona-Malik equation of a small thickness K. Observe that a Perona-Malik equation of a large thickness K will diffuse the edge before removing all the noise. Consequently, if the objective is segmentation, it is best to use as small a value of K as possible. Following the procedure prescribed by Perona, Shiota, and Malik in [4], we computed the histogram of the absolute values of the gradient throughout the initial signal, and fixed K at 10% of its integral. The resulting evolution is shown in Figure 7. In addition to its good denoising performance, it also blurs the edge, which is clearly undesirable if the objective is a sharp segmentation. The comparison of Figures 6 and 7 strongly suggests that the smaller K the better. It was precisely this observation that originally motivated the development of SIDEs. However, while in 1-D a SIDE evolution can be viewed precisely as a limit of a Perona-Malik evolution as K goes to

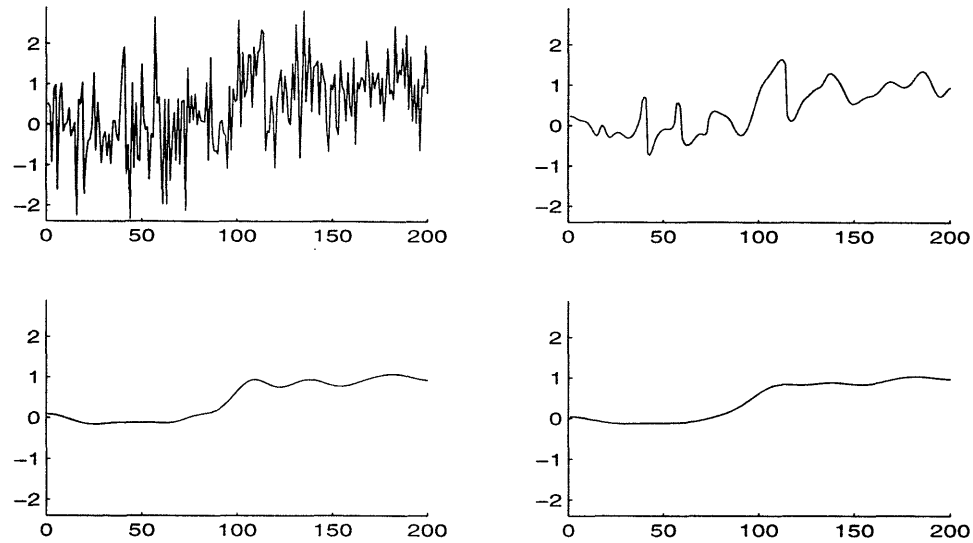

Figure 7: Scale space of a Perona-Malik equation with a large K for a noisy step of Figure 6.

0, there is still an advantage to using the form of the evolution that we have described, rather than a Perona-Malik evolution with a very small value of K. Specifically, the presence of explicit reductions in dimensionality during the evolution makes a SIDE implementation more efficient than that described in [4]. Even for this simple example the Perona-Malik evolution that produced the result comparable to that in Figure 6 evolved approximately 5 times more slowly than our SIDE evolution. Although a SIDE in 2-D cannot be viewed as a limit of Perona-Malik evolutions, the same comparison in speed of evolution is still valid, with the difference in computation time being orders of magnitude in this case.

4.2 Experiment 2: SIDE Evolutions in 2-D

In the 2-D example, shown in Figure 8, we see that if allowed to evolve until exactly two regions are left, the SIDE produces the most important boundary in the image. This property is used to advantage in segmenting a SAR image in which only two textures are present (forest and grass). The initial SAR image and the scale space are shown in Figure 8, and the resulting boundary is superimposed onto the original image in Figure 9. SAR imagery, such as the example shown here, are subject to the phenomenon known as speckle, which is present in any coherent imaging system and which leads to the large amplitude variations and noise evident in the original image. Consequently, the accurate segmentation of such imagery can be quite challenging and in particular cannot be accomplished using standard edge detection algorithms. In contrast, the two-region segmentation displayed in Figure 9 is extremely accurate.

Finally we note, that, as mentioned in Experiment 1, the SIDE evolutions require far less computation time than Perona-Malik-type evolutions. Since in 2-D a SIDE evolution is not a limiting form of a Perona-Malik evolution, the comparison is not quite as simple. However, in experiments that we have performed in which we have devised Perona-Malik evolutions that produce results as qualitatively similar to those in Figure 8 as possible, we have found that the resulting computational effort is roughly 130 times slower for this (201×201) image than our SIDE evolution.

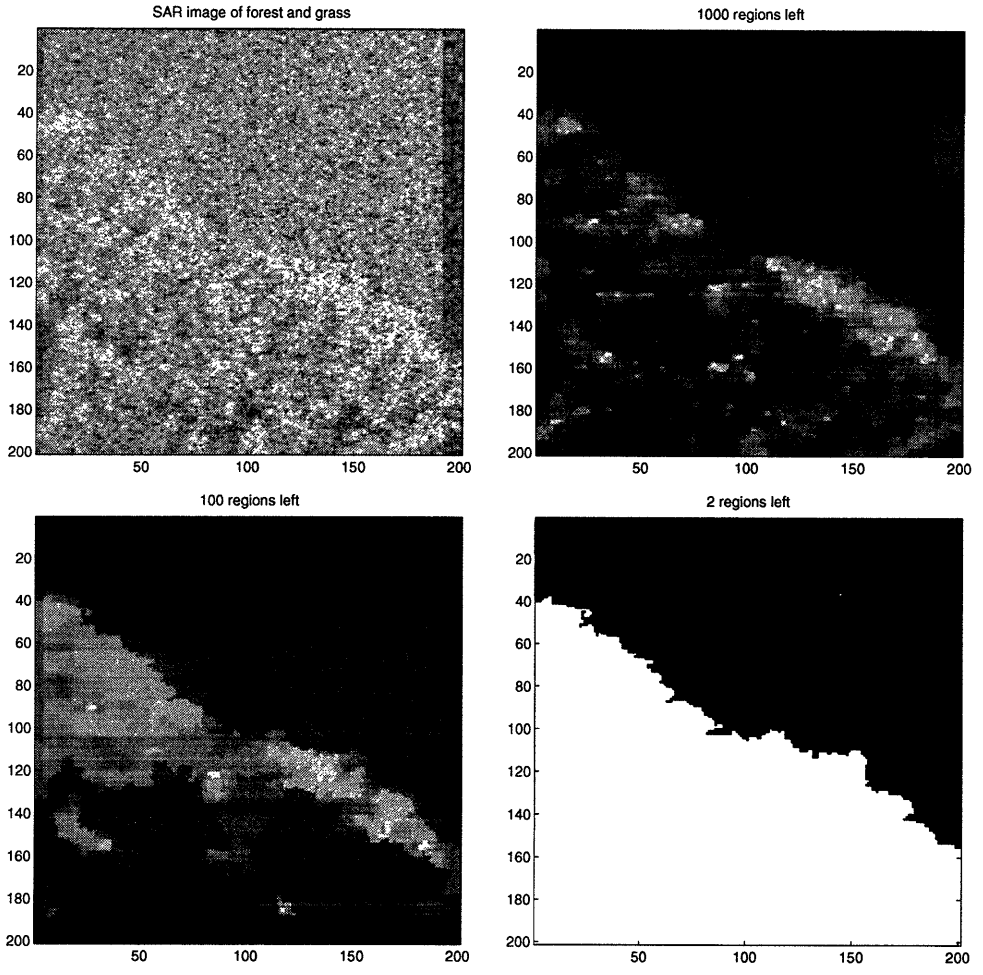

Figure 8: Scale space of a SIDE for the SAR image of trees and grass.

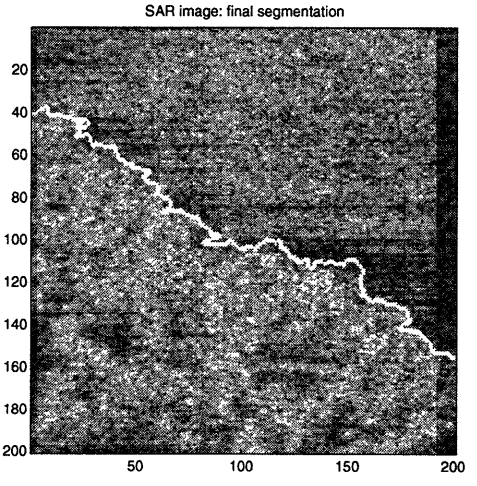

Figure 9: The final boundary superimposed on the initial SAR image.

5 Conclusion

In this paper we have presented a new approach to edge enhancement and segmentation and demonstrated its successful application to signals and images with very high levels of noise. Our approach is based on a new class of evolution equations for the processing of imagery and signals which we have termed stabilized inverse diffusion equations or SIDEs. These evolutions, which have discontinuous right-hand sides, have conceptual and mathematical links to other evolution-based methods in signal and image processing, but they also have their own unique qualitative characteristics and properties that, together with the promising results presented here, suggest the merit of several further lines of investigation, described in [5].

References

[1] T. Lindeberg. *Scale-Space Theory in Computer Vision.* Kluwer Academic Publishers, 1994.

[2] J.-M. Morel and S. Solimini. *Variational Methods in Image Segmentation.* Birkhauser, 1995.

[3] P. Perona and J. Malik. Scale-space and edge detection using anisotropic diffusion. *IEEE Trans. on PAMI*, 12(7), 1990.

[4] P. Perona, T. Shiota, and J. Malik. Anisotropic diffusion. In [6].

[5] I. Pollak, A. S. Willsky, and H. Krim. Image segmentation and edge enhancement with stabilized inverse diffusions. LIDS Technical Report 2368, Laboratory for Information and Decision Systems, MIT, 1996. Submitted to *IEEE Trans. on Image Processing.*

[6] B.M. ter Haar Romeny, editor. *Geometry-Driven Diffusion in Computer Vision.* Kluwer Academic Publishers, 1994.

[7] V.I. Utkin. *Sliding Modes in Control and Optimization.* Springer-Verlag, 1992.

[8] J. Weickert. Nonlinear diffusion scale-spaces: from the continuous to the discrete setting. In *ICAOS: Images, Wavelets, and PDEs*, pages 111–118, Paris, 1996.